Eur. J. Mech. B - Fluids 19 (2000) 831–854

S0997-7546(00)00132-1/FLA

Large-scale vortex structures in shear flows

Viktor P. Goncharov [a], Vadim I. Pavlov [b,*]

[a] *Institute of Atmospheric Physics, Russian Academy of Sciences, 109017 Moscow, Russia*
[b] *DMF, UFR de Mathématiques Pures et Appliquées, Université de Lille 1, 59655 Villeneuve d'Ascq cedex, France*

(Received 10 March 1999; revised 6 July 1999 and 29 March 2000; accepted 5 April 2000)

Abstract – This article considers the developments of the Hamiltonian Approach to problems of fluid dynamics, and applies the general method to strongly non-linear large-scale vortex structures in shear flows. Such vortex structures can appear in shear flows like Poiseulle and Couette flows. The Hamiltonian version of contour dynamics for two-dimensional layer models in a constant-density ideal fluid has be developed. The Hamiltonian description is formulated in terms of the dynamic variables with KdV-type Poisson brackets. The use of the method of pseudo-differential operators permits the regular application of approximation methods. Thus, governing equations can be easily derived correctly in any order of perturbation theory. We discuss also the effect of vortex structures on the average velocity profile of the flows. © 2000 Éditions scientifiques et médicales Elsevier SAS

large-scale vortex structures / shear flows / Hamiltonian Approach

1. Introduction

Large-scale, long-lived vortex structures attract the particular interest of scientists because of the role these phenomena play in transporting momentum, mass and energy in the atmosphere and ocean. Such objects are found in many types of hydrodynamic flows and possess a wide variety of generation mechanisms. The vortex structures can be driven by various causes or combination of causes, among which are shear, density stratification, viscosity, heat conductivity and others, including nonlinearity. Strong nonlinearity manifests itself especially sharply in generating spatially isolated vortex structures.

The present work is devoted to the study of two-dimensional large-scale vortex structures in incompressible homogeneous ideal flows, neglecting everything except shear. Such idealization is justified in many real flows, including turbulent ones, if the characteristic scale of the structures is greater than the scale of turbulent pulsations, and viscosity acts only on the background flow. In such models, effectively inviscid and non-turbulent, the influence of viscosity and turbulence on the structures can be indirectly parameterized via the shear of the background flow. For example, in this fashion the boundary layer formation, or the flattening effect of turbulence on the velocity profile in a pipe, may be parameterized.

Two-dimensional flows with ultra-high Reynolds numbers have the striking property of organizing spontaneously into large scale coherent vortex structures. The well-known example is of Jupiter's Great Red Spot, a huge vortex persisting for more three centuries in a turbulent shear between two zonal jets.

The assumption of large scales allows us to make several radical simplifications. First, we restrict our consideration to such two-dimensional flows where the continuous velocity profile can be replaced by a layer model with constant vorticity in each layer. Such a model is valid when large-scale motions are weakly sensitive to a fine structure of the velocity profile. In this scenario one may expect that even crude approximations,

* Correspondence and reprints.

with a small number of layers, describing only the general structure of the real velocity profile grasp large-scale dynamics qualitatively correctly. Secondly, as we demonstrate subsequently, the layer models allow us to formulate the dynamics of the flow in terms of interfaces, determining the contours of the vortex structures, within the framework of spatially one-dimensional integro-differential nonlinear equations.

The equations of contour dynamics describe the self-induced motion of vorticity – discontinuity boundaries, or 'contours', in an inviscid, incompressible, two-dimensional fluid whose vorticity distribution is piecewise constant. From a physical viewpoint the approximation made seems too severe. But detailed comparisons between contour dynamics and a conventional numerical simulation (see for example Zabusky et al. [1], Saffman [2], Dritchel [3], Dritschel and McIntyre [4] and references therein) have shown surprisingly good agreement for flows with distributed vorticity at hight Reynolds number. It appears that many aspects of nearly inviscid flows with continuous, distributed vorticity can be reproduced using contour dynamics with a moderate number of vorticity levels. These results suggest that contour dynamics may be a competitive analytical tool in certain problems of scientific interest, particularly in connection with large scale, very high Reynolds number flows in ocean and atmospheres of planets.

The Hamiltonian formulation developed in the works of Goncharov and Pavlov [5,6] is most convenient not only for deriving the contour dynamics equations, but also for estimating the extent to which one or the other of the approximations used is universal. The method also allows one to reduce analytical manipulations to a minimum when solving concrete problems. Indeed, in this approach the object of the approximating procedures is not the dynamic equations which are typically large in number, but a single quantity – the Hamiltonian. In addition, the Hamiltonian approach allows us to overcome the barrier of weak nonlinearity. Notice that the required approximation procedure may be developed if the parameter of nonlinearity is defined as a ratio between the transverse and longitudinal sizes of the vortex structure.

The results of the analytical consideration presented below may serve, on the one hand, as a theoretical guideline for qualitative experimental estimates, and on the other, to assist in more accurate numerical modeling. In this regard in should be noted that, frequently, brute-force computer calculations of nonlinear vortex and wave phenomena for complex configurations may not be very reliable. Often such results depend on a number of factors of secondary importance which distort the overall picture by introducing features frequently even nonexistent. Thus, the 'the big picture' of the phenomenon must be always thoroughly taken to consideration.

In the following section we outline the key points of the general approach of the application of the Hamiltonian formulation to the two-dimensional layer models. Section 3 applies the Hamiltonian Approach to vortex structures in Poiseuille-type flows. The method is applied to vortex structures in Couette-type flows in section 4. In conclusion, we review the results and highlight the features of the application of the Hamiltonian formalism to the considered two-dimensional non-linear large-scale vortex structures in shear flows.

2. General approach

2.1. Contour dynamics in Hamiltonian description

Let us consider the dynamics of incompressible flows governed by the equations

$$\partial_t v_\alpha + v_\beta \partial_\beta v_\alpha = \partial_\alpha(\rho^{-1} p), \quad \partial_\beta v_\beta = 0, \tag{1}$$

where v_α are velocity components ($\alpha, \beta = 1, 2, 3$) in the Cartesian system of coordinates, ∂_t is the partial derivative of a field variable with respect to time, p is pressure, ρ is density (further $\rho = 1$). The summation convention is implied on repeated Greek indices when tensor notation is used. As is well known (Arnold [7]; Morrison [8]; Goncharov and Pavlov [5,6]), the system (1) may be presented on the phase space of the vorticity field

$$\Omega_\alpha = \varepsilon^{\alpha\mu\beta}\partial_\mu v_\beta \tag{2}$$

($\varepsilon^{\alpha\mu\beta}$ is the Levi-Civita tensor) in Hamiltonian form as

$$\partial_t \Omega_\alpha = \{\Omega_\alpha, H\} = \int \mathrm{d}\mathbf{x}' \{\Omega_\alpha, \Omega'_\beta\} \frac{\delta H}{\delta \Omega'_\beta}. \tag{3}$$

Here and from now on, prime denotes that the field variables depend on space coordinate $\mathbf{x}'$. The functional $H = H[\mathbf{\Omega}]$ under the symbol of the variational derivative $\delta/\delta\Omega_j$, the kinetic energy of flow:

$$H = \frac{1}{2}\int \mathrm{d}\mathbf{x}\mathbf{v}^2, \tag{4}$$

is the Hamiltonian. Here and further, $\mathrm{d}\mathbf{x} = \mathrm{d}x_1\,\mathrm{d}x_2\,\mathrm{d}x_3$.

The skew-symmetric functional Poisson bracket in equation (3), $\{\Omega(\mathbf{x}), \Omega(\mathbf{x}')\}$, is local and is defined for the given model by expression

$$\{\Omega_\alpha, \Omega'_\beta\} = \varepsilon^{\alpha\sigma\kappa}\varepsilon^{\kappa\lambda\nu}\varepsilon^{\beta\nu\mu}\partial_\sigma \Omega_\lambda \partial_\mu \delta(\mathbf{x} - \mathbf{x}'). \tag{5}$$

The Hamiltonian structure of the system consists of the Hamiltonian given by the total energy and the functional Poisson bracket $\{\cdot,\cdot\}$. Conservation of energy follows from the given formulation of governing equations, since $\partial_t H = \{H, H\} = 0$.

Let us recall here a few definitions (Morse and Feshbach [9]).

For orthogonal, curvilinear coordinates q_1, q_2, q_3 with unit vectors $\mathbf{e}_1, \mathbf{e}_2, \mathbf{e}_3$, line element $\mathrm{d}l^2 = g_{ij}\,\mathrm{d}q^i\,\mathrm{d}q^j$, $g_{ij} = h^2_{(i)}\delta_{ij}$, $g = g_{11}g_{22}g_{33}$, and scale factors $h_{(i)}$, the differential operators applicated to a vector field $\mathbf{F}$ become

$$(\nabla\cdot\mathbf{F}) = g^{-1/2}\frac{\partial}{\partial q^n}\left(g^{1/2}h^{-1}_{(n)}F_n\right), \quad (\mathrm{curl}\,\mathbf{F})_i = h_{(i)}g^{-1/2}\epsilon_{ijk}\frac{\partial}{\partial q^j}\left(h_{(k)}F_k\right). \tag{6}$$

Here, $F_i = (\mathbf{e}_i \cdot \mathbf{F})$.

If F_n are the components of an ordinary vector $\mathbf{F}$ in a tree-dimensional orthogonal system of coordinates with scale factors h_n, then the quantities $f_n = h_n F_n$ are said to be the ‘covariant’ components of a vector in the same coordinate system and the quantities $f^n = F_n/h_n$ are called the ‘contravariant’ components of a vector in the same system. Therefore, if f_n are the components of a covariant vector, then $f^n = f_n/h_n^2$ are the corresponding components of the contravariant vector in the same coordinate system. The covariant f_i and contravariant components f^i of ‘physical’ vector $\mathbf{F}$ coincide only in Euclidean space, when $g_{11} = g_{22} = g_{33} = 1$. In a curvilinear space, the contravariant component is derived from covariant one according to the following well-known procedure: $f_i = g_{ik}f^k$, or $f^i = g^{ik}f_k$, etc. When the g_{ik}-tensor components are not dimensionless, dimensions of f^i and f_i differ naturally. The different components do not have the same dimensionality; if an ordinary vector $\mathbf{F}$ has the dimensions of length, for example, then the components of the corresponding contravariant vector have dimension equal to the dimensions of the associated coordinate and the dimensions of the covariant components have still other dimensions.

Letting

$$\Omega^\alpha = g^{-1/2}\varepsilon^{\alpha\beta\kappa}\partial_\beta v_\kappa, \tag{7}$$

the curvilinear generalization of (4) and (5) to the case when the coordinates used $\mathbf{x} = (x_1, x_2, x_3)$ are not Cartesian may be written (see Gonharov and Pavlov [5]) as

$$\{\Omega^\alpha, \Omega'^\beta\} = g^{-1/2}\varepsilon^{\alpha\sigma\kappa}\varepsilon^{\kappa\lambda\nu}\varepsilon^{\beta\nu\mu}\partial_\sigma\Omega_\lambda\partial_\mu g^{-1/2}\delta(\mathbf{x}-\mathbf{x}'), \tag{8}$$
$$H = \frac{1}{2}\int \mathrm{d}\mathbf{x} g^{1/2} g^{\alpha\beta} v_\alpha v_\beta,$$

where $g_{\alpha\beta}$ is the metric tensor, g is its determinant, Ω^α are contravariant components of the vorticity, v_α are covariant components of the hydrodynamocal velocity, etc.

We will effectively consider two-dimensional incompressible flows whose particles moves along non intersecting stationary fluid surfaces. Depending on the symmetry of the problem, it is convenient to study such flows in a suitable system of orthogonal curvilinear coordinates x_1, x_2, x_3 so that coordinate lines x_3 coincide with vortex ones while coordinate lines x_1 and x_2 lay on the fluid surfaces. In such a coordinate system the vector field of the velocity has two covariant components, v_1, v_2, only, and the vector field of the vorticity has one component, $(\operatorname{curl}\mathbf{v})_3$. In this case, $\boldsymbol{\Omega} = \{0, 0, \Omega\}$, where $\Omega = g^{-1/2}(\partial_1 v_2 - \partial_2 v_1)$. By virtue of the incompressibility condition $\operatorname{div}\mathbf{v} = g^{-1/2}\partial_n(g^{1/2}h_{(n)}^{-2}v_n) = 0$, these quantities can be expressed in terms of the stream function Ψ as

$$v_1 = g_{11}g^{-1/2}\partial_2\Psi, \qquad v_2 = -g_{22}g^{-1/2}\partial_1\Psi; \tag{9}$$
$$\Omega = -g^{-1/2}(\partial_1 g_{22}g^{-1/2}\partial_1 + \partial_2 g_{11}g^{-1/2}\partial_2)\Psi. \tag{10}$$

In two-dimensional case the Poisson bracket (8) reduces to the more simple expression:

$$\{\Omega, \Omega'\} = \frac{\varepsilon^{\alpha\beta}}{\sqrt{g}}\frac{\partial\Omega}{\partial x_\alpha}\frac{\partial}{\partial x_\beta}\frac{\delta(\mathbf{x}-\mathbf{x}')}{\sqrt{g}} \quad (\alpha, \beta = 1, 2). \tag{11}$$

To avoid confusion, it should be remind that the dimension of contravariant component of vorticity, Ω, named further merely as vorticity, can differ from one of the 'usual' vorticity $(\operatorname{curl}\mathbf{v})_3$ which is connected with Ω by the relationship $(\operatorname{curl}\mathbf{v})_3 = \Omega g^{1/2}(g_{11}g_{22})^{-1/2}$. Both definitions coincide in cases when $g = g_{11}g_{22}$, or $h_{(3)} = 1$.

The fundamental nature of the contravariant vorticity Ω is based on the fact that in two-dimensional incompressible non-plane flows this characteristic is just a scalar quantity which obeys to the law

$$\partial_t\Omega + v^\alpha\partial_\alpha\Omega = 0 \quad (\alpha = 1, 2).$$

That is, Ω is conserved conveying fluid particles along their Lagrangian trajectories. For this reason, it plays so important role in the covariant generalization of the 'contour-dynamics method' and makes it possible to reduce the two-dimensional dynamics of layers with constant vorticity to the dynamics of interfaces, thus lowering the dimensionality of the problem by one. Motion equations for Ω allow one to develop methods of contour-dynamics in a natural way.

Without the loss of generality we assume that x_1 coincides with streamlines of the unperturbed stationary problem. For this wide class of layer models geometric properties of the space associated with such coordinate systems are characterized only by components g_{11}, g_{22}, g_{33} of the metric tensor and by its determinant g which are deemed independent of x_1, just as the velocity profile of the unperturbed flow.

As said above, we restrict our consideration to layer models with constant vorticity in each layer. The vorticity distribution of N-layer model can be written in general form as

$$\Omega = \omega_1\theta(L_0 - x_2) + \sum_{i=1}^{N-1}(\omega_{i+1} - \omega_i)\theta(\eta_i - x_2) - \omega_N\theta(L_N - x_2), \tag{12}$$

where $x_2 = L_0$, $x_2 = L_N$ are exterior rigid boundaries $(L_0 < L_N)$, $\eta_i = \eta_i(x_1, t)$ are dynamical variables which describe shape of the layer boundaries $(\eta_{i+1} > \eta_i)$, ω_i is the constant contravariant vorticity of the i-th layer sandwiched between the i-th and $(i+1)$-th interfaces; θ-function is defined by

$$\theta(x) = \begin{cases} 1, & x \geqslant 0; \\ 0, & x < 0. \end{cases}$$

The representation of the vorticity in terms of θ-functions allows us to transform the Poisson bracket (11) to the form

$$\{\theta_i, \theta_k'\} = \frac{\delta_{ik}\varepsilon^{\alpha\beta}}{\nu_i\sqrt{g}} \frac{\partial\theta_i}{\partial x_\alpha} \frac{\partial}{\partial x_\beta} \frac{\delta(\mathbf{x} - \mathbf{x}')}{\sqrt{g}} \quad (\alpha, \beta = 1, 2; i = 1, \ldots, N-1), \tag{13}$$

where $\theta_i = \theta(\eta_i - x_2)$, $\nu_i = \omega_{i+1} - \omega_i$ is the vorticity jump at i-th boundary, δ_{ik} is the Kronecker symbol. To obtain Poisson brackets convenient for describing of contour dynamics models, we introduce new dynamical variables:

$$\kappa_i = \int g^{1/2}\big[\theta(\eta_i - x_2) - \theta(-x_2)\big]\,\mathrm{d}x_2 = \int_0^{\eta_i} g^{1/2}\,\mathrm{d}x_2. \tag{14}$$

Corresponding Poisson brackets for the variables κ_i are derived directly from (13) by the following way:

$$\{\kappa_i, \kappa_k'\} = \int\!\!\int g^{1/2} g'^{1/2}\{\theta_i, \theta_k'\}\,\mathrm{d}x_2\,\mathrm{d}x_2' = -\frac{\delta_{ik}}{\nu_i}\frac{\partial}{\partial x_1}\delta(x_1 - x_1'). \tag{15}$$

It should be emphasized that result (14), (15) is exact and is obviously independent on any approximations made in the Hamiltonian H.

Thus we can describe an evolution of contours in the above layer model in the framework of the Hamiltonian formulation as

$$\partial_t\kappa_i = \{\kappa_i, H\} = -\frac{1}{\nu_i}\partial_1\frac{\delta H}{\delta\kappa_i}. \tag{16}$$

Since the Hamiltonian H coincides with the kinetic energy of the flow, in terms of the full stream function it can be expressed in the following form

$$H = \frac{1}{2}\int \mathrm{d}x_1\,\mathrm{d}x_2\,g^{-1/2}\sum_{n=1}^{N}(\theta_i - \theta_{i-1})\big[g_{11}(\partial_2\Psi_i)^2 + g_{22}(\partial_1\Psi_i)^2\big], \tag{17}$$

where $\Psi_i = \psi_i^0 + \psi_i$ is the full stream function of the i-th layer, $\eta_0 = L_0$ and $\eta_N = L_N$. In equilibrium, a layer-wise vorticity-homogeneous model is a set of layers separated by interfaces $x_2 = l_i = \text{const}$. Then the unperturbed stream functions ψ_i^0 corresponding to a continuous profile of the flow velocity are determined as solutions of the following boundary value problem

$$\begin{gathered} \partial_2 g_{11} g^{-1/2}\partial_2\psi_i^0 = -g^{1/2}\omega_i, \\ \big[\psi_{i+1}^0 - \psi_i^0\big]_{x_2 = l_i} = 0, \qquad \big[\partial_2(\psi_{i+1}^0 - \psi_i^0)\big]_{x_2 = l_i} = 0. \end{gathered} \tag{18}$$

Note that in the more general case when N-layer two-dimensional flow is piecewise constant not only in a vorticity but also in a density the Hamiltonian contour dynamics for a given i is described not by one variable, but two variables. Various versions of Poisson brackets for such models were found by Goncharov and Pavlov [5].

It is desirable to formulate the problem in terms of the counter variables only. There are two ways to determine H explicitly and exactly, in terms of η_i, and hence in terms of κ_i, without resorting to the traditional approximation of weak nonlinearity. Both of the ways are related to the approaches to solving the boundary value problem of finding perturbation of the stream function ψ_i

$$\left(\partial_1 g_{22} g^{-1/2} \partial_1 + \partial_2 g_{11} g^{-1/2} \partial_2\right) \psi_i = 0, \tag{19}$$

$$[\psi_{i+1} - \psi_i]_{x_2=\eta_i} = \left[\psi_i^0 - \psi_{i+1}^0\right]_{x_2=\eta_i}, \tag{20}$$

$$\left[\partial_1(\psi_{i+1} - \psi_i)\right]_{x_2=\eta_i} = 0, \tag{21}$$

where (20) and (21) are the velocity continuity conditions. One must also add the conditions of vanishing normal components of the fluid velocity at the exterior rigid boundaries $x_2 = L_0$, $x_2 = L_N$ $(L_0 < L_N)$, if these exist:

$$\psi_1|_{x_2=L_0} = \psi_i|_{x_2=L_N} = 0. \tag{22}$$

The first method is the Green function method. The second method is the method of pseudo-differential operators. This method will be used in this work. Effectively, both ways, the Green function method and the method of pseudo-differential operators are equivalent. Note that the one-to-one correspondence between pseudo-differential operators and integral transformations allows us, if desired, to reinterpret the results obtained in one form in terms of the other.

2.2. *Method of pseudo-differential operators*

Within the framework of the method of pseudo-differential operators (Maslov [10]), it is convenient to construct the Hamiltonian in three steps. In the first step, the general solution (19) is written as

$$\psi_i = F_1(x_2, \Gamma) A_i + F_2(x_2, \Gamma) B_i, \qquad \Gamma = \partial_1 \hat{H}, \tag{23}$$

$$\hat{H} f(x_1) = \frac{1}{\pi} \int_{-\infty}^{+\infty} \frac{f(x_1')}{x_1 - x_1'} \, \mathrm{d}x_1', \tag{24}$$

where Γ is the Hilbert transform operator, $\hat{H}$, followed by the differentiation with respect to x_1, and A_i and B_i are some functions of x_1.

The action of pseudo-differential operator $F(x_2, \Gamma)$ is equivalent to the integral transformation

$$F(x_2, \Gamma) f(x_1) = \frac{1}{2\pi} \int F\left(x_2, |k|\right) \mathrm{e}^{ik(x-x_1)} f(x) \, \mathrm{d}x \, \mathrm{d}k, \tag{25}$$

and is unambiguously determined by function $F(x_2, |k|)$ named by the symbol of the pseudo-differential operator. As a result, by substituting (25) directly into (19) we find that symbols of operators F_1 and F_2 appearing in (23) are linearly independent solutions of the equation

$$\left(\partial_2 g_{11} g^{-1/2} \partial_2 - k^2 g_{22} g^{-1/2}\right) F_{1,2}\left(x_2, |k|\right) = 0. \tag{26}$$

After determining F_1 and F_2, the next step is to find functions A_i and B_i. Substituting (23) in boundary conditions (20)–(22) yields a set of equations for defining functions A_i and B_i

$$\begin{aligned} &F_1(\eta_i, \Gamma)[A_{i+1} - A_i] + F_2(\eta_i, \Gamma)[B_{i+1} - B_i] = \left[\psi_i^0 - \psi_{i+1}^0\right]_{x_2=\eta_i}, \\ &F_1(\eta_i, \Gamma)\partial_1[A_{i+1} - A_i] + F_2(\eta_i, \Gamma)\partial_1[B_{i+1} - B_i] = 0, \\ &F_1(L_0, \Gamma) A_1 + F_2(L_0, \Gamma) B_1 = 0, \qquad F_1(L_N, \Gamma) A_N + F_2(L_N, \Gamma) B_N = 0. \end{aligned} \tag{27}$$

To calculate these functions for non-commutative operators Γ and $\eta_i(x_1)$ we follow the rule of ordering these operators: the operators act in the order from the right to the left. Hereinafter such a rule allows us to distinguish conjugated operators $F(\eta_i,\Gamma)$ and $F(\Gamma,\eta_i)=F^+(\eta_i,\Gamma)$. Operator $F(\eta_i,\Gamma)$ implies that the first to be acted on is operator Γ, and the operator of multiplication by $\eta_i(x_1)$ acts second. Operator $F(\Gamma,\eta_i)$ implies conversely that the operator of multiplication by $\eta_i(x_1)$ acts first, and operator Γ acts second. It should be noted that operators $F(\eta_i,\Gamma)$ and $F(\Gamma,\eta_i)$ are equivalent to different integral transformations (Maslov [10])

$$F(\eta_i,\Gamma)f(x_1)=\frac{1}{2\pi}\int F\bigl(\eta_i(x_1),|k|\bigr)\exp\bigl(ik(x-x_1)\bigr)f(x)\,\mathrm{d}x\,\mathrm{d}k, \tag{28}$$

$$F(\Gamma,\eta_i)f(x_1)=\frac{1}{2\pi}\int F\bigl(\eta_i(x),|k|\bigr)\exp\bigl(ik(x-x_1)\bigr)f(x)\,\mathrm{d}x\,\mathrm{d}k. \tag{29}$$

Before presenting the solution of system (27) which is constructed using the method of non-commutative operators, we introduce the following operator symbols:

$$\begin{aligned}
&D(|k|)=g_{11}g^{-1/2}(F_2\partial_2F_1-F_1\partial_2F_2),\qquad P=F_2^NF_1^0-F_1^NF_2^0,\\
&F_{1,2}^0=F_{1,2}|_{x_2=L_0},\qquad F_{1,2}^N=F_{1,2}|_{x_2=L_N},\\
&S_{1,2}=\int_0^{x_2}F_{1,2}\bigl(x_2,|k|\bigr)g^{1/2}\,\mathrm{d}x_2.
\end{aligned} \tag{30}$$

Here all symbols excluding $S_{1,2}$ do not depend on x_2. Next we introduce definitions

$$\begin{aligned}
&S_{1,2}^i=S_{1,2}(\eta_i,\Gamma)-S_{1,2}(l_i,\Gamma),\qquad S_{1,2}^{i+}=S_{1,2}(\Gamma,\eta_i)-S_{1,2}(\Gamma,l_i),\\
&U_0^i=\nu_i\bigl(S_1^iF_2^0-S_2^iF_1^0\bigr),\qquad U_N^i=\nu_i\bigl(S_1^iF_2^N-S_2^iF_1^N\bigr),\\
&U_0^{i+}=\nu_i\bigl(F_2^0S_1^{i+}-F_1^0S_2^{i+}\bigr),\qquad U_N^{i+}=\nu_i\bigl(F_2^NS_1^{i+}-F_1^NS_2^{i+}\bigr).
\end{aligned} \tag{31}$$

In terms of (30) and (31) solutions for A_i and B_i take the form

$$\begin{aligned}
A_i&=-\frac{1}{PD}\sum_{n=1}^{N-1}\bigl[\theta(n-i)F_2^0U_N^{n+}+\theta(i-1-n)F_2^NU_0^{n+}\bigr],\\
B_i&=\frac{1}{PD}\sum_{n=1}^{N-1}\bigl[\theta(n-i)F_1^0U_N^{n+}+\theta(i-1-n)F_1^NU_0^{n+}\bigr].
\end{aligned} \tag{32}$$

Here $\theta(m)$ is the Heaviside function equal to one if $m\geqslant 0$ and to zero if $m<0$.

Using (23) and (32), the Hamiltonian (17) may be expressed in terms of layer interfaces η_i

$$\begin{aligned}
H=-\frac{1}{2}\int\mathrm{d}x_1\Biggl\{\sum_{n=1}^{N-1}\Biggl[\nu_n\int_0^{\eta_n}g^{1/2}\bigl(\psi_{n+1}^0+\psi_n^0\bigr)\,\mathrm{d}x_2\\
-2\frac{\gamma_0}{P}U_N^{n+}+2\frac{\gamma_N}{P}U_0^{n+}\Biggr]-\sum_{n,i=1}^{N-1}U_0^n\frac{\sigma_{ni}}{PD}U_N^{i+}\Biggr\},
\end{aligned} \tag{33}$$

where we have used notations

$$\gamma_0=\psi_1^0|_{x_2=L_0},\qquad \gamma_N=\psi_N^0|_{x_2=L_N},\qquad \sigma_{ni}=\theta(i-n)+\theta(i-1-n).$$

Two important comments must be made regarding Hamiltonians of the N-layer models. The first follows from the fact that in the starting formulation the fluid models are homogeneous in the x_1-direction of the coordinate space. Hence, the motion equations have to be invariant under Galileo's transformation $x_1' = x_1 - ct$, $t' = t$, where c is a constant parameter. Then, according to this property, the Hamiltonian (17) has to be invariant under the transformation $v^{1\prime} = v^1 - c$ for the contravariant components of velocity v^1. Since $v^1 = g^{-1/2}\partial_2\psi$, in terms of stream functions, it means an invariance under the transformation

$$\psi' = \psi - c\int_{c_0}^{x_2} g'^{-1/2}\,\mathrm{d}x_2'.$$

Two arbitrary parameters c and c_0 of the given invariant transformation make it possible to choose without loss of generality the stream function so that $\psi_1^0|_{x_2=L_0} = \gamma_0 = 0$ and $= \psi_N^0|_{x_2=L_N} = \gamma_N = 0$.

Galileo's symmetry for the dynamic models like (16) leads to the invariant of motion

$$I_0 = \int_{-\infty}^{+\infty}\sum_{i=1}^{N-1}\nu_i\kappa_i^2\,\mathrm{d}x_1,$$

which can be found from (16) directly with using Galileo's transformation. Other invariants are conditioned solely by the structure of the Poisson brackets

$$I_i = \int_{-\infty}^{+\infty}\kappa_i\,\mathrm{d}x_1$$

and named as Casimirs. According to the motion equations (16), the determination of the Hamiltonian with an accuracy to these invariants give no effect on the dynamics except trivial translation with a constant velocity.

Secondly, the Hamiltonian (33) does not depend on a choice of equilibrium parameters l_i and may be reformulated in terms of solely dynamic variables η_i. Introducing of parameters l_i implies a priori information about a background regime of the flow or about its equilibrium state. It may be convenient when an expansion of the Hamiltonian in the perturbation theory series around the equilibrium is used. Note that if in Hamiltonian (33) we make the separately summation of terms which depend on l_i, then their total contribution will be expressed through an linear combination of the motion integrals $I_0, I_1, \ldots, I_{N-1}$.

2.3. Plane-parallel models

Plane-parallel flows are most conveniently described in the Cartesian coordinate system. In this case, $x_1 = x$, $x_2 = z$, $x_3 = y$, $g_{11} = g_{22} = g_{33} = 1$. In equilibrium, the flow consists of a set of plane-parallel layers which are demarcated by interfaces $z = l_i$. Equilibrium stream function ψ_i^0, dynamic variable κ_i and operators F_1, F_2, D, P, S_1, S_2 required to construct the Hamiltonian are given by

$$\begin{aligned}
&\psi_i^0 = -\omega_i\frac{z^2}{2} + \alpha_i z + \sigma_i, \qquad \alpha_{i+1} - \alpha_i = \nu_i l_i, \qquad \sigma_{i+1} - \sigma_i = -\nu_i\frac{l_i^2}{2};\\
&\kappa_i = \eta_i;\\
&F_1 = \exp(-z\Gamma), \qquad F_2 = \exp(z\Gamma),\\
&D = -2\Gamma, \qquad P = 2\sinh(L_N - L_0)\Gamma,\\
&S_1 = \bigl(1 - \exp(-z\Gamma)\bigr)\Gamma^{-1}, \qquad S_2 = -\bigl(1 - \exp(z\Gamma)\bigr)\Gamma^{-1}.
\end{aligned} \tag{34}$$

As an illustration, we give the derivation of Hamiltonian for the two-layer model when the layer of uniform vorticity adjacent to a rigid wall so that the corresponding non-perturbed distribution of vorticity is

$\omega=\omega_0,\ 0<z<h$, and $\omega=0,\ h<z<\infty$. Note that an analogous model was used for numerical simulations of steepening and filamentation phenomena (Pullin [11]).

According to (34) the non-perturbed stream functions for such model are

$$\psi_1^0=-\omega_0\frac{z^2}{2},\qquad \psi_2^0=-\omega_0 h\left(z-\frac{h}{2}\right). \tag{35}$$

The operators D, P, U_0, U_N^+ needed to construct the Hamiltonian are calculated from (30) and (31), which give to leading order as $L_0=0, L_N\to\infty$:

$$D=-2\Gamma,\qquad P=F_2^N,$$
$$U_0=-2\omega_0\big[\cosh(h\Gamma)-\cosh(\eta\Gamma)\big]\frac{1}{\Gamma},\qquad U_N^+=-\omega_0\frac{F_2^N}{\Gamma}\big[\exp(-\Gamma h)-\exp(-\Gamma\eta)\big]. \tag{36}$$

Substituting (35) and (36) in (33), one obtains after some algebra in terms of the interface $\eta(x,t)$ (the contribution from terms with γ_0 and γ_N being zero as $L_0=0, L_N\to\infty$),

$$H=-\frac{\omega_0^2}{2}\int_{-\infty}^{\infty}\left\{\frac{1}{3!}\eta^3+\frac{h}{2!}\eta^2-\big[\cosh(h\Gamma)-\cosh(\eta\Gamma)\big]\frac{1}{\Gamma^3}\big[\exp(-\Gamma h)-\exp(-\Gamma\eta)\big]\right\}\mathrm{d}x, \tag{37}$$

where constant terms and terms linear in η are neglected since they have no effect on the dynamics.

For large-scale approximations it is more convenient to rewrite (37) in the form independent on the parameter h characterizing the non-perturbed regime. Expansion into formal infinite power series permits us compute the following operator expressions

$$\big[\cosh(h\Gamma)-1\big]\frac{1}{\Gamma^3}\big[1-\exp(-\Gamma\eta)\big]=\left[\frac{1}{2!}h^2\Gamma^2+\cdots\right]\frac{1}{\Gamma^3}\left[\Gamma\eta-\frac{1}{2!}\Gamma^2\eta^2+\cdots\right]=\frac{1}{2!}h^2\eta+\partial_x(\cdots),$$
$$\big[\exp(-h\Gamma)-1\big]\frac{1}{\Gamma^3}\big[1-\cosh(\Gamma\eta)\big]=\left[-h\Gamma+\frac{1}{2!}h^2\Gamma^2+\cdots\right]\frac{1}{\Gamma^3}\left[\frac{1}{2!}\Gamma^2\eta^2+\cdots\right]=-\frac{1}{2!}h\eta^2+\partial_x(\cdots), \tag{38}$$

where $\partial(\cdots)$ denotes terms whose integral with respect to x vanishes as, by definition, η and its derivatives become zero at infinity. Using (38) and rearranging terms in (37), we can eliminate terms with h and find

$$H=-\frac{\omega_0^2}{2}\int_{-\infty}^{\infty}\left\{\frac{1}{3!}\eta^3-\big[1-\cosh(\eta\Gamma)\big]\frac{1}{\Gamma^3}\big[1-\exp(-\Gamma\eta)\big]\right\}\mathrm{d}x. \tag{39}$$

As more general result, we present the reduced Hamiltonian for the plane N-layer model. Corresponding procedure is realized by the same scheme as for (39). Finally, by omitting the terms linear in η which do not make contribution to the motion equation, after some rearrangement (the terms dependent of parameters l_i of the non-perturbation problem cancel out), we obtain from (33)

$$H=\frac{1}{2}\int_{-\infty}^{+\infty}\mathrm{d}x_1\left\{\sum_{n=1}^{N-1}\nu_n\left[\frac{\omega_{n+1}+\omega_n}{3!}\eta_n^3-\frac{\omega_N L_N^2-\omega_1 L_0^2}{2(L_N-L_0)}\eta_n^2\right]\right.$$
$$\left.-\sum_{n,i=1}^{N-1}\big[\cosh L_0\Gamma-\cosh(L_0-\eta_n)\Gamma\big]\frac{\nu_n\nu_i\sigma_{ni}}{\Gamma^3\sinh(L_N-L_0)\Gamma}\big[\cosh\Gamma L_N-\cosh\Gamma(L_N-\eta_n)\big]\right\}. \tag{40}$$

2.4. *Plane ring models*

Plane ring models are naturally described in polar coordinates. Therefore, $x_1=\varphi$, $x_2=\rho$, $x_3=z$, $g_{11}=g=\rho^2$, $g_{22}=g_{33}=1$. In equilibrium, the flow is presented as a set of concentric ring layers which are demarcated by interfaces $\rho = l_i$. The flow in such a model is characterized by stream functions

$$\psi_i^0 = -\omega_i \frac{\rho^2}{4} + \alpha_i \ln\frac{\rho}{R} + \sigma_i, \qquad \alpha_{i+1} - \alpha_i = \nu_i \frac{l_i^2}{2}, \qquad \sigma_{i+1} - \sigma_i = \nu_i \frac{l_i^2}{4}\left(1 - 2\ln\frac{l_i}{R}\right). \tag{41}$$

Here, R is some fixed quantity taken to account for the proper dimensionality.

In this model dynamic variable κ_i and operators $F_1,\ F_2,\ D,\ P,\ S_1,\ S_2$ required to construct the Hamiltonian have the following form

$$\begin{aligned}
&\kappa_i = \int_0^{\eta_i} \rho\,\mathrm{d}\rho = \frac{\eta_i^2}{2};\\
&F_1 = \left(\frac{\rho}{R}\right)^{-\Gamma}, \qquad F_2 = \left(\frac{\rho}{R}\right)^{\Gamma},\\
&D = -2\Gamma, \qquad P = \left(\frac{L_N}{L_0}\right)^{\Gamma} - \left(\frac{L_0}{L_N}\right)^{\Gamma},\\
&S_1 = \rho^2\left(\frac{\rho}{R}\right)^{-\Gamma}\frac{1}{2-\Gamma}, \qquad S_2 = \rho^2\left(\frac{\rho}{R}\right)^{\Gamma}\frac{1}{2+\Gamma}.
\end{aligned} \tag{42}$$

It is necessary to take into account the fact that the polar angle φ is a cyclical coordinate. Then formula (24) for the Hilbert transform incorporated in operator $\Gamma = \partial_\varphi \hat{H}$ should be replaced with

$$\hat{H} f(\varphi) = \frac{1}{2\pi}\int_{-\pi}^{\pi} f(\varphi')\cot\left(\frac{\varphi - \varphi'}{2}\right)\mathrm{d}\varphi'.$$

In the special case $N = 2,\ L_0 = 0,\ L_2 = \infty,\ \omega_1 = \omega_0,\ \omega_2 = 0,\ l_1 = R$, we have the model of a circular patch of radius R containing vorticity ω_0 embedded in unbounded irrotational fluid. According to (41) the non-perturbed stream functions for such model are

$$\psi_1^0 = -\omega_0\frac{\rho^2}{4}, \qquad \psi_2^0 = -\omega_0\frac{R^2}{4}\left[\ln\left(\frac{\rho}{R}\right)^2 - 1\right]. \tag{43}$$

The operators D, P, U_0, U_N^+ needed to construct the Hamiltonian are calculated from (42), (30) and (31), which give to leading order as $L_0 \to 0$, $L_N \to \infty$:

$$\begin{aligned}
&D = -2\Gamma, \qquad P = F_2^N F_1^0,\\
&U_0 = \omega_0 R^2\left[\left(\frac{\eta}{R}\right)^{2+\Gamma} - 1\right]\frac{F_1^0}{2+\Gamma}, \qquad U_N^+ = -\omega_0 R^2 \frac{F_2^N}{2-\Gamma}\left[\left(\frac{\eta}{R}\right)^{2-\Gamma} - 1\right]^+.
\end{aligned} \tag{44}$$

Here sign $+$ means that corresponding operator expression should be reordered in accordance with the rule formulated above. Substituting (43) and (44) in (33), one obtains after some algebra in terms of the dynamic variable η (the contribution from terms with γ_0 and γ_N being zero as $L_0 \to 0$, $L_N \to \infty$),

$$H = -\frac{\omega_0^2 R^4}{4}\int_{-\pi}^{\pi}\left\{\frac{1}{8}\left(\frac{\eta}{R}\right)^4 + \frac{1}{2}\left(\frac{\eta}{R}\right)^2\ln\frac{\eta}{R} - \left[\left(\frac{\eta}{R}\right)^{2+\Gamma} - 1\right]\frac{1}{\Gamma(4-\Gamma^2)}\left[\left(\frac{\eta}{R}\right)^{2-\Gamma} - 1\right]^+\right\}\mathrm{d}\varphi, \tag{45}$$

where constant terms and terms linear in $\kappa = \eta^2/2$ are excluded since they have no effect on the dynamics (see remarks in the end of section 2.2).

2.5. Weakly nonlinear approximation

Let us show that the exact Hamiltonian (45) leads to correct limit cases.

The simplest case of the weakly nonlinear evolution of a uniform circular vortex patch has been considered, in the framework of traditional classical approach, by Dritschel [3]. The comparison between our result and one of Dritschel [3] seems be quite important as, according to Saffman [2], the Hamiltonian could be worked out only approximately and its nature was not established exactly. Our result – the explicit formula (45) shows that the Hamiltonian is the total energy of the flow.

So, let us consider a weakly nonlinear approximation of the Hamiltonian when disturbances at the boundary are small $((\eta - R)/R \ll R)$. In terms of the variable

$$q = \frac{1}{2}(\eta^2 - R^2), \tag{46}$$

from (45) by expanding the operator expressions into power series we obtain to quartic order in q:

$$H_4 = -\frac{\omega_0^2}{4}\int_{-\pi}^{\pi}\left\{q^2 - q\frac{1}{\Gamma}q - \frac{1}{3R^2}q^3 + \frac{1}{3R^4}q^4 - \frac{1}{R^4}\left(\frac{1}{3}q\Gamma q^3 - \frac{1}{4}q^2\Gamma q^2\right)\right\}\mathrm{d}\varphi. \tag{47}$$

It follows from (15) and (46) the Poisson bracket for q is

$$\{q, q'\} = \frac{1}{\omega_0}\frac{\partial}{\partial\varphi}\delta(\varphi - \varphi'). \tag{48}$$

Thus, the equation of motion is found from

$$\partial_t q = \{q, H_4\} = \frac{1}{\omega_0}\frac{\partial}{\partial\varphi}\frac{\delta H_4}{\delta q}, \tag{49}$$

and can be written as

$$\partial_t q = \frac{\omega_0}{2}\frac{\partial}{\partial\varphi}\left\{-q + \frac{1}{\Gamma}q + \frac{1}{2R^2}q^2 - \frac{2}{3R^4}q^3 + \frac{1}{6R^4}\left(\Gamma q^3 - 3q^2\Gamma q - 3q\Gamma q^2\right)\right\}. \tag{50}$$

The obtained equation may be easily reformulated in terms of integral transformations if we take into account that

$$\hat{H}^2 = -1, \qquad \partial_\varphi\frac{1}{\Gamma}f(\varphi) = \frac{1}{\hat{H}}f(\varphi) = -\hat{H}f(\varphi),$$

and

$$\Gamma f(\varphi) = \frac{1}{2\pi}\partial_\varphi\int_{-\pi}^{\pi} f(\varphi')\cot\left(\frac{\varphi - \varphi'}{2}\right)\mathrm{d}\varphi' = -\frac{1}{2\pi}\int_{-\pi}^{\pi}\frac{f(\varphi')\,\mathrm{d}\varphi'}{1 - \cos(\varphi - \varphi')}.$$

Using these integral representations for operators $\partial_\varphi\Gamma^{-1}$ and Γ, the equation (50) can be rewritten as

$$\partial_t q + \frac{\omega_0}{2}\left(\frac{\partial q}{\partial\varphi} + \hat{H}q\right) = \omega_0\frac{\partial}{\partial\varphi}\left(\frac{1}{4R^2}q^2 - \frac{1}{3R^4}q^3 + \frac{1}{24\pi R^4}\int_{-\pi}^{\pi}\frac{(q - q')^3\,\mathrm{d}\varphi'}{1 - \cos(\varphi - \varphi')}\right). \tag{51}$$

The equation (51) has be obtained by Marsden and Weinstein [12] (without cubic nonlinear terms) and by Dritschel (with cubic nonlinear terms) [3] (see also Saffman ([2], p. 177–178) beginning from classical equations of the fluid dynamics. It follows from the general expression (45) as the simplest case.

2.6. Axisymmetrical models

Axially symmetric fluid motions are reasonably considered in the cylindrical coordinate system. Then $x_1 = z$, $x_2 = \rho$, $x_3 = \varphi$, $g_{11} = g_{22} = 1$, $g_{33} = g = \rho^2$. In correspondence with (18) for such a model equilibrium, stream function ψ_i^0 and operators F_1, F_2, D, P, S_1, S_2 are defined by expressions utilizing the Hamiltonian expressed in terms of dynamic variable κ_i

$$\begin{aligned}
&\psi_i^0 = -\omega_i \frac{\rho^4}{8} + \alpha_i \rho^2 + \sigma_i, \qquad \alpha_{i+1} - \alpha_i = \nu_i \frac{l_i^2}{4}, \qquad \sigma_{i+1} - \sigma_i = -\nu_i \frac{l_i^4}{8};\\
&\kappa_i = \int_0^{\eta_i} \rho \, \mathrm{d}\rho = \frac{\eta_i^2}{2};\\
&F_1 = \rho I_1(\rho\Gamma), \qquad F_2 = \rho K_1(\rho\Gamma), \qquad D = 1,\\
&P = L_N L_0 \left[K_1(L_N\Gamma) I_1(L_0\Gamma) - K_1(L_0\Gamma) I_1(L_N\Gamma)\right],\\
&S_1 = \rho^2 I_2(\rho\Gamma)\Gamma^{-1}, \qquad S_2 = -\left[\rho^2 K_2(\rho\Gamma) - 2\Gamma^{-2}\right]\Gamma^{-1},
\end{aligned} \tag{52}$$

where I_1 and I_2 are the modified Bessel functions of the first-kind, respectively of the first and the second order, while K_1 and K_2 are the modified Bessel functions of the second kind, respectively of the first and the second order (Abramovitz and Stegun [13]).

2.7. Ring models on sphere

Two-dimensional motions on a sphere are conveniently described in the spherical coordinate system. Assuming without the loss of generality that the sphere radius is equal to one, the coordinates and the components of the metric tensor become $x_1 = \varphi$, $x_2 = \vartheta$, $x_3 = 1$, $g_{22} = 1$, $g_{11} = g = \sin^2\vartheta$. In equilibrium, unperturbed interfaces divide the sphere into vorticity-homogeneous layers $\vartheta = l_i (0 \leqslant \vartheta \leqslant \pi)$, so that the corresponding equilibrium stream function ψ_i^0 is determined by

$$\begin{aligned}
&\psi_i^0 = \omega_i \ln\sin\vartheta + \alpha_i \ln\tan\frac{\vartheta}{2} + \sigma_i, \qquad \alpha_{i+1} - \alpha_i = -\nu_i \cos l_i, \qquad (53)\\
&\sigma_{i+1} - \sigma_i = -\nu_i \left[\ln\sin l_i - (\cos l_i) \ln\tan\frac{l_i}{2}\right].
\end{aligned}$$

In this case dynamic variable κ_i and operators F_1, F_2, D, P, S_1, S_2 are defined as

$$\begin{aligned}
&\kappa_i = \int_0^{\eta_i} \sin\vartheta \, \mathrm{d}\vartheta = 1 - \cos\eta_i; \qquad (54)\\
&F_1 = \left(\tan\frac{\vartheta}{2}\right)^{-\Gamma}, \qquad F_2 = \left(\tan\frac{\vartheta}{2}\right)^{\Gamma},\\
&D = -2\Gamma, \qquad P = \left(\frac{\tan(L_N/2)}{\tan(L_0/2)}\right)^{\Gamma} - \left(\frac{\tan(L_0/2)}{\tan(L_N/2)}\right)^{\Gamma},\\
&S_1 = \frac{8(\sin\frac{\vartheta}{2})^{2-\Gamma}}{2-\Gamma} {}_2F_1\left(-\frac{\Gamma}{2}, 1 - \frac{\Gamma}{2}, 2 - \frac{\Gamma}{2}; \sin^2\frac{\vartheta}{2}\right),\\
&S_2 = \frac{8(\sin\frac{\vartheta}{2})^{2+\Gamma}}{2+\Gamma} {}_2F_1\left(\frac{\Gamma}{2}, 1 + \frac{\Gamma}{2}, 2 + \frac{\Gamma}{2}; \sin^2\frac{\vartheta}{2}\right),
\end{aligned}$$

where ${}_2F_1(\alpha, \beta, \gamma; z)$ is the hyper-geometric function (Abramovitz and Stegun [13]).

3. Vortex structures in Poiseuille-type flow

3.1. Model Hamiltonians in large-scale approximation: cylindrical and plane cases

Within the framework of the layer models vortex structures appear as solutions describing rather strong modulations of vorticity-homogeneous layers. In general, the modulation effect has several regimes. Some of them give rise to solitary vortices with a fixed structure and propagation speed (Goncharov [14]).

It is well known that under a constant pressure gradient a laminar viscous flow in a round pipe – the so-called axially-symmetric Poiseuille flow – is characterized by a parabolic velocity profile (Landau and Lifshitz [15]). From the standpoint of the axially-symmetric layer models considered in section 2.6 such a flow represents a constant-vorticity cylindrical layer which is unable to evolve because the boundary of the layer is fixed by the rigid wall of the pipe. The situation reverses as soon as the flow becomes turbulent and its average profile flattens. In the first approximation one may attempt to describe this effect within the framework of the two-layer model using the biparabolic approximation for the velocity profile of the background flow

$$v = \begin{cases} (\omega_2/2)\big(a^2 - \rho^2\big), & l \leqslant \rho \leqslant a; \\ (\omega_1/2)\big(l^2 - \rho^2\big) + (\omega_2/2)\big(a^2 - l^2\big), & 0 \leqslant \rho \leqslant l; \end{cases} \tag{55}$$

where ω_1 and ω_2 are contravariant components of vorticities of the inner and outer (boundary) layer, respectively, a is the pipe radius, l is the radius of the inner layer (see section 3.3). Let us recall that in axisymmetrical case the dimension the contravariant component of vorticity, Ω, is $length^{-1} time^{-1}$.

In contrast to the one-layer model, the two-layer model is dynamically non-degenerate and admits formation of vortex structures. According to (33) and (52) the Hamiltonian of such a model may be presented as (see Goncharov and Pavlov [5])

$$H = -\frac{1}{2}\int_{-\infty}^{+\infty} \mathrm{d}x \left\{ \frac{\nu_1}{2}\left[\frac{\omega_2 a^2}{8}\eta_1^4 - \frac{\omega_1+\omega_2}{4!}\eta_1^6\right] + \nu_1^2\eta_1^2 I_2(\eta_1\Gamma)\Gamma^{-2} \right.$$
$$\left. \times \left[\frac{K_1(a\Gamma)}{I_1(a\Gamma)} I_2(\Gamma\eta_1) + K_2(\Gamma\eta_1) - 2\Gamma^{-2}\eta_1^{-2}\right]\eta_1^2 \right\}, \tag{56}$$

where $\nu_1 = \omega_2 - \omega_1$ is the vorticity jump at the boundary $\rho = \eta_1(x_1, t)$. For the cylindrical model we can choose the length-scale L and the time-scale T as

$$L = a, \qquad T = \frac{8}{a\nu_1}. \tag{57}$$

Then it is convenient to introduce non-dimensional variables $q = (\eta_1/a)^2$, $\xi = x/a$, $\tau = t/T$ in terms of which the motion equation takes form

$$\partial_\tau q = -\partial_\xi \frac{\delta E}{\delta q}, \tag{58}$$

where E is the non-dimensional Hamiltonian of the cylindrical two-layer model defined as

$$E = 32a^{-7}\nu_1^{-2} H. \tag{59}$$

By expanding the modified Bessel functions into power series and considering the terms of the first and the second order in q_ξ (i.e., rather large-scale perturbations), we obtain

$$E = \frac{1}{2}\int_{-\infty}^{+\infty} \mathrm{d}\xi \left[q^2(q-1-\ln q)q_\xi^2 + q^4 + \alpha_3 q^3 + \alpha_2 q^2\right], \tag{60}$$

where the coefficients α_3 and α_2 are given by

$$\alpha_3 = \frac{4}{3}\frac{\omega_1 - 2\omega_2}{\omega_2 - \omega_1}, \qquad \alpha_2 = 2\frac{\omega_2}{\omega_2 - \omega_1}. \tag{61}$$

The structure of the non-dimensional Hamiltonian (60) turns out to be sufficiently universal.

In the plane model with the unperturbed velocity profile, which is more simple mathematically,

$$v = \begin{cases} \omega_2(h-z), & l \leqslant z \leqslant h; \\ \omega_1(l-z) + \omega_2(h-l), & 0 \leqslant z \leqslant l; \\ \omega_1(l+z) + \omega_2(h-l), & -l \leqslant z \leqslant 0; \\ \omega_2(h+z), & -h \leqslant z \leqslant -l; \end{cases}$$

the Hamiltonian for symmetric large-scale perturbations exhibits the same qualitative character. Here, the vorticities $\omega_{1,2}$ have the dimension $time^{-1}$.

The corresponding model can be considered as a four-layer approximation of a plane Poiseuille flow (Landau and Lifshitz [15]) in a channel with width $2h$ (see *figure 1*).

For the plane model the length and time scales are chosen as

$$L = h, \qquad T = \frac{4}{\nu_1}. \tag{62}$$

Using the results of section 2.3 it is easy to show that for symmetric perturbations $(\eta_3 = -\eta_1, \eta_2 = 0)$ in terms of the non-dimensional variables $q = \eta_1/h = -\eta_3/h$, $\tau = t/T$, the exact Hamiltonian of the given model is

$$H = \frac{1}{2}\nu_1^2 h^4 \int_{-\infty}^{+\infty} \mathrm{d}\xi \left\{\frac{1}{3!}\frac{\omega_2+\omega_1}{\omega_2-\omega_1}q^3 - \frac{1}{4}\frac{\omega_2+\omega_1}{\omega_2-\omega_1}q^2 - [1-\cosh q\Gamma]\frac{1}{\Gamma^3 \sinh\Gamma}\left[1-\cosh\Gamma(1-q)\right]\right\}. \tag{63}$$

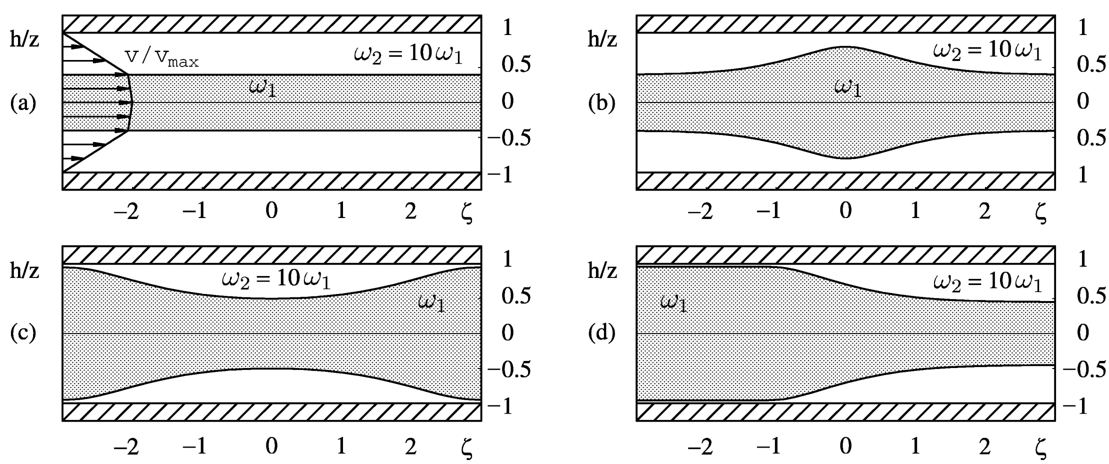

Figure 1. Wave-like vortex structures in the plane four-layer model: (a) the model of unperturbed flow with piecewise linear velocity profile; (b) solitary wave-like perturbation of negative polarity; (c) solitary wave-like perturbation of negative polarity; (d) shock-wave solution.

The evolution of q is described by the same equation (58) if the non-dimensional Hamiltonian E is defined as $E=-2h^{-4}\nu_1^{-2}H$. In the same approximation as (60), from (63) after a some algebra we have

$$E=\frac{1}{2}\int_{-\infty}^{+\infty}\mathrm{d}\xi\left[\frac{4}{3}q^2(q-1)^2q_\xi^2+q^4+\alpha_3q^3+\alpha_2q^2\right]. \tag{64}$$

It is remarkable that the non-dimensional Hamiltonians (60) and (64) for the plane and cylindrical models are similar and also that the dimensionless coefficients α_2 and α_3 are universally defined by (61).

3.2. Equations of motion: solution classification

We will seek stationary solutions of equation (58) in the form $q(\zeta)$ where $\zeta=\xi-c\tau$ and c is the propagation speed. In this case, equation (58) with Hamiltonian (64) is integrated two times. As a result, we obtain the following ordinary differential equation:

$$\frac{4}{3}q^2(q-1)^2q_\zeta^2=q^4+\alpha_3q^3+(\alpha_2-c)q^2+\alpha_1q+\alpha_0=(q-q_1)(q-q_2)(q-q_3)(q-q_4). \tag{65}$$

Here, α_1 and α_0 are integration constants and q_i $(i=1,2,3,4)$ are the roots of the fourth-order polynomial appearing on the right-hand side of (65). Then

$$q_1+q_2+q_3+q_4=-\alpha_3, \tag{66}$$

$$q_1q_2+q_1q_3+q_1q_4+q_2q_3+q_2q_4+q_3q_4=\alpha_2-c. \tag{67}$$

It follows from equation (65), that physically meaningful solutions exist only if all the q_i-roots are real and satisfy the inequality $q_1\leqslant q_2\leqslant q_3\leqslant q_4$. Thus, the middle roots, q_2 and q_3, setting the upper and the lower bounds of the solution, lie in the range between zero and one, i.e.,

$$0\leqslant q_2\leqslant q\leqslant q_3\leqslant 1.$$

We commence with the case when all the q_i-roots are distinct. In this case the corresponding solutions of (65) have a periodical character and can be expressed in terms of elliptic functions. Flow incompressibility imposes the condition:

$$\int_0^T(p-q)\,\mathrm{d}\zeta=\frac{4}{\sqrt{3}}\int_{q_2}^{q_3}\frac{(p-q)q(1-q)}{\sqrt{(q-q_1)(q-q_2)(q-q_3)(q-q_4)}}\,\mathrm{d}q=0, \tag{68}$$

where T is a period of the solution and $p=l/a$ is a parameter. Integral equality (68) together with (67), in principle, allows us to express the velocity c as a function of parameters $\omega_1,\omega_2,q_1,q_2,p$.

In the case of multiple roots there exist three variants of the solution. In the first variant, by assuming that

$$p=q_1=q_2\leqslant q\leqslant q_3<q_4,$$

we obtain the following solution:

$$|\zeta|=\frac{2}{\sqrt{3}}\Bigg\{\sqrt{(q_3-q)(q_4-q)}+(2+\alpha_3)\ln\left[\sqrt{q_3-q}+\sqrt{q_4-q}\right]$$
$$+\frac{p(1-p)}{\sqrt{(q_3-p)(q_4-p)}}\ln\left[\frac{\sqrt{(q_3-q)(q_4-p)}+\sqrt{(q_4-q)(q_3-p)}}{(q-p)(q_4-q_3)}\right]\Bigg\}, \tag{69}$$

which as shown in *figure 1(b)* presents a solitary wave-like perturbation of positive polarity with amplitude $A = q_3 - p > 0$.

The second variant implies that

$$q_1 < q_2 \leqslant q \leqslant q_3 = q_4 = p.$$

For this case the solution is given by

$$|\zeta| = \frac{2}{\sqrt{3}}\Big\{\sqrt{(q-q_1)(q-q_2)} + (2+\alpha_3)\ln\big[\sqrt{q-q_1} + \sqrt{q-q_2}\big] + \frac{p(1-p)}{\sqrt{(q_3-p)(q_4-p)}}\ln\left[\frac{\sqrt{(q-q_1)(p-q_2)} + \sqrt{(q-q_2)(p-q_1)}}{(p-q)(q_2-q_1)}\right]\Big\}, \tag{70}$$

and corresponds to a solitary wave-like perturbation of negative polarity with amplitude $A = q_2 - p < 0$ (see *figure 1(c)*). Asymptotically, at $|\zeta| \to \infty$, both solutions (69) and (70) follow the behavior of the unperturbed problem $q = p$. It is possible to show that these solutions exist in the domain of values A and p which lie between $A = 0$ and $A = -2p - \alpha_3/2$.

The third and last variant is illustrated in *figure 1(d)* and is realized when

$$0 < q_1 = q_2 \leqslant q \leqslant q_3 = q_4 < 1, \quad p = (q_1 + q_2)/2.$$

In this case solutions resemble shock waves and are described by

$$\zeta = \frac{2}{\sqrt{3}}\Big\{-q + \frac{q_2+q_3}{2} + \frac{q_3(1-q_3)}{q_3-q_2}\ln\left[2\frac{q_3-q}{q_3-q_2}\right] + \frac{q_2(1-q_2)}{q_3-q_2}\ln\left[2\frac{q-q_2}{q_3-q_2}\right] + \frac{p(1-p)}{\sqrt{(q_3-p)(q_4-p)}}\ln\left[\frac{\sqrt{(q-q_1)(p-q_2)} + \sqrt{(q-q_2)(p-q_1)}}{(p-q)(q_2-q_1)}\right]\Big\}. \tag{71}$$

3.3. Solitary vortex structures

The case of pairwise merging of the roots when $q = 0, 1$ deserves separate consideration. In principle, the corresponding solutions can be obtained by taking the limit $p \to 0$ in solution (69), limit $p \to 1$ in (70), and $q_2 \to 0$, $q_3 \to 1$ in (71). However, to obtain solutions of a more general form we should turn directly to equation (65).

For example, to find a general solution for $q_1 = q_2 = 0$ we write down equation (65) as

$$q^2\left[\frac{4}{3}(q-1)^2 q_\zeta^2 - (q-q_3)(q-q_4)\right] = 0. \tag{72}$$

From (72) it follows that the general solution represents piecewise-continuous function obtained by ‘sewing’ together the particular solution, $q = 0$, and the solution of the equation

$$q_\zeta^2 = \frac{3}{4}(q-1)^{-2}(q-q_3)(q-q_4), \tag{73}$$

which may alternate arbitrarily. Such a solution appears as an arbitrary sequence of isolated dipole vortex structures. As shown in *figure 2(a)* the shape of the structures determined by (73) is symmetric with respect to the ζ-axis of the channel and resembles a ‘cat’s eye’.

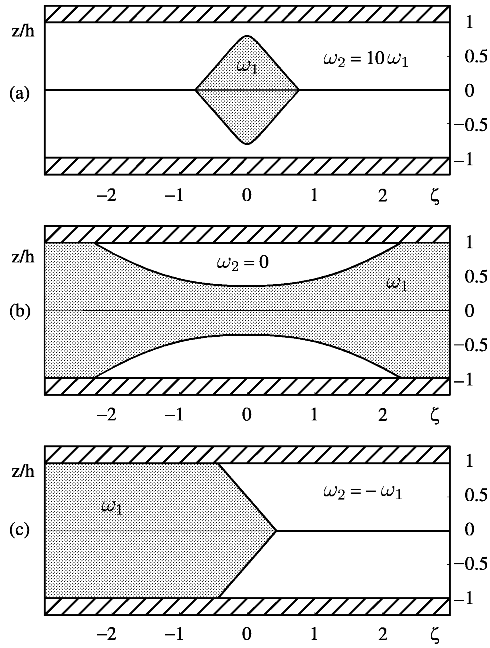

Figure 2. Limit-form vortex structures in the plane four-layer model: (a) isolated vortex structure of central type; (b) wall vortex structure; (c) cork-like vortex structure.

The case where $q_3 = q_4 = 1$ can be considered analogously. It can be seen in *figure 2(b)* that the solutions form isolated vortex structures adjoining the channel walls. As expected from the symmetry of the problem and may be verified directly, the description is invariant with respect to the change of variables

$$q \to 1 - q, \quad q_i \to 1 - q_i, \quad \zeta \to -\zeta, \quad \omega_1 \to \omega_2, \quad \omega_2 \to \omega_1. \tag{74}$$

For this reason, the required solutions can be derived by substituting (74) in the case above. Notice that in the reference frame moving at the average velocity of the background flow, when all other parameters are equal, both central and wall vortex structures are characterized by the propagation velocities equal in value, but opposite in direction.

In the simplest case when $q_1 = q_2 = 0$, $q_3 = q_4 = 1$, equation (69) takes the form

$$q^2(q-1)^2\left(\frac{4}{3}q_\zeta^2 - 1\right) = 0, \tag{75}$$

and has the solutions

$$q = 0, \qquad q = 1, \qquad q = \pm\frac{2}{\sqrt{3}}\zeta + \text{const}. \tag{76}$$

These solutions are used as the basis for constructing dipole vortex structures which occupy all the cross-section of the channel. According to (67) such structures have the vorticity opposite to the vorticity of the background flow $\omega_1 = -\omega_2$ and are immobile, $c = 0$. Based on solutions (76) it is possible to construct a structure acting in the flow like a ‘jam’. Note that found solutions may be considered as the simplest model of turbulent clusters observed in a turbulent flow in a pipe with Reynolds numbers greater than 3200 (Kantwell [16]).

Solutions of cylindrical model (60) with biparabolic flow profile (55) can be analyzed and classified in an analogous way. The toroidal vortex structures arising in such a flow are described by

$$\begin{aligned} q^2(q-1-\ln q)q_\zeta^2 &= q^4+\alpha_3 q^3+(\alpha_2-c)q^2+\alpha_1 q+\alpha_0 \\ &= (q-q_1)(q-q_2)(q-q_3)(q-q_4). \end{aligned} \tag{77}$$

Equation (77) differs from (65) only by the left side which has a substantially different behavior in the neighborhood of $q=0$. This distinction most strongly manifests itself for solutions varying in the range that includes point $q=0$. Therefore, it is sufficient to consider (77) when $q_1=q_2=0$. In this case, equation (77) splits and its general solution can be obtained by a piecewise continuous ‘sewing’ of two equations

$$q=0, \qquad q_\zeta^2=\frac{(q-q_3)(q-q_4)}{q-1-\ln q}. \tag{78}$$

If, in addition, $q_3=q_4=1$, the general solution becomes a combination of the solutions of these three equations:

$$q=0, \qquad q=1, \qquad q_\zeta^2=\frac{(1-q)^2}{q-1-\ln q}. \tag{79}$$

The corresponding vortex structures are shown in *figure 3*. *Figures 3(b)* and *(c)* show, respectively, the shapes of the isolated, central and wall, vortex structures. Structures (79) presented in *figure 3(d)* look like a ‘cork’. According to (67) they are immobile, $c=0$, and their vorticity is opposite to the vorticity of the background flow, $\omega_1=-\omega_2$.

The non-dimensional propagation speed, c, of the vortex structures can be found from (67) when all remaining parameters are fixed. In particular, for vortex structures (73), (78) with $q_1=q_2=0$, it follows from (67) that

$$c=q_3^2+\alpha_3 q_3+\alpha_2. \tag{80}$$

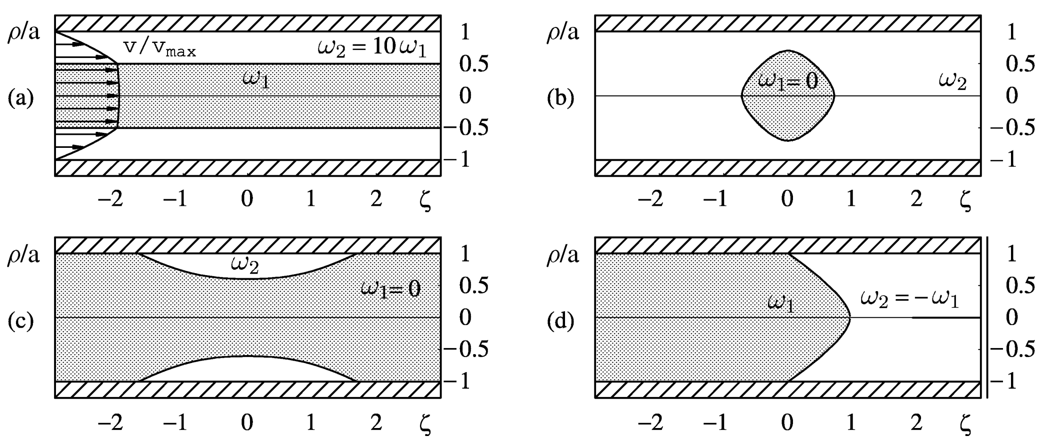

Figure 3. Limit-form vortex structures in the cylindrical two-layer model: (a) the model of unperturbed flow with biparabolic velocity profile; (b) isolated vortex structure of central type; (c) wall vortex structure; (d) cork-like vortex structure.

If we take $\omega_2 = 0$, $\omega_1 = \omega$ and $q_3 = (R/a)^2 \ll 1$, from (80) we find $c \approx -\frac{4}{3}(R/a)^2$. Recalculation of c in the dimensional presentation in accordance with the scales (57) gives for the propagation speed

$$u = c\frac{L}{T} = c\frac{a^2\nu_1}{8} = \frac{1}{6}\omega R^2. \tag{81}$$

It is interesting to note that this expression for the propagation speed is in a good agreement with the Hill vortex (Milne-Thomson [17]). Recall that the Hill vortex, which represents an exact solution of the equations of fluid dynamics, is a vorticity-homogeneous ($\omega = \text{const}$) spherical vortex of radius R, moving in immovable fluid with constant speed

$$u_H = \frac{2}{15}\omega R^2.$$

The developed approach can also be applied to many other physical situations. In general, the derived equations of contour dynamics can be nonlocal, as, for example, in the vorticity-homogeneous cylindrical layer simulating a body wake or a fluid-penetrating jet. The corresponding Hamiltonian of this model can be obtained from (56) by applying $a \to \infty$ and then the large-scale approximation $l/\lambda < 1$.

4. Vortex structures in Couette-type flow

4.1. Hamiltonian formulation of the model

In this section we consider large-scale vortex structures in the shear flow with the average velocity profile typical of a turbulent Couette flow. As will be demonstrated, spatially periodic stationary vortex structures of various types may form is such a flow. We will also analyze the effect of these vortex structures on the average flow profile.

It is well known that Couette flow realized between two parallel walls moving in opposite directions with identical speeds is characterized in the turbulent regime by a particular velocity profile. The profile is flat in the center of the channel and bends steeply near the walls (Landau and Lifshitz [15]). The equivalent three-layer vorticity-homogeneous model that possesses the necessary qualitative properties is characterized by the following velocity profile:

$$v = \begin{cases} -\Omega l + \omega(l - z), & l \leqslant z \leqslant h; \\ -\Omega z, & -l \leqslant z \leqslant l; \\ \Omega l + \omega(l - z), & -h \leqslant z \leqslant -l. \end{cases} \tag{82}$$

Here ω's are the vorticities of the wall (boundary) layers, h is the channel half-width, l is the half-width of the unperturbed inner layer with vorticity Ω (see *figure 4(a)*).

According to (40), in terms of variables η_1 and η_2 describing the interfaces which demarcate the layers, the Hamiltonian H takes the form

$$\begin{aligned} H = \frac{(\Omega-\omega)^2}{2}\int_{-\infty}^{+\infty}\bigg\{&\frac{1}{3!}\frac{\Omega+\omega}{\Omega-\omega}\left(\eta_1^3 - \eta_2^3\right) - \left[\cosh h\Gamma - \cosh(h+\eta_1)\Gamma\right] \\ &\times \frac{1}{\Gamma^3\sinh 2h\Gamma}\left[\cosh(h-\eta_1)\Gamma - \cosh(h-\eta_2)\Gamma\right] + \left[\cosh h\Gamma - \cosh(h-\eta_2)\Gamma\right] \\ &\times \frac{1}{\Gamma^3\sinh 2h\Gamma}\left[\cosh(h+\eta_1)\Gamma - \cosh(h+\eta_2)\Gamma\right]\bigg\}\,\mathrm{d}x, \end{aligned} \tag{83}$$

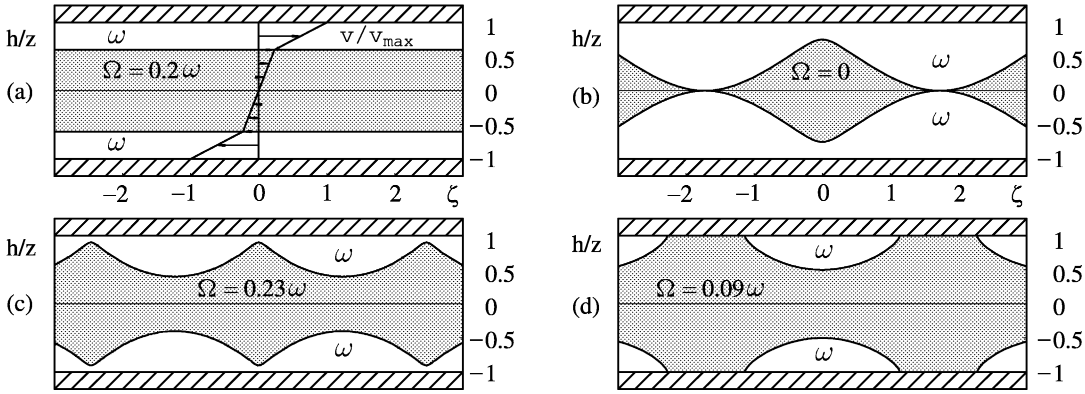

Figure 4. Stationary periodic vortex structures in the plane three-layer model of Couette flow: (a) the model of unperturbed flow with piecewise linear velocity profile for $\Omega = 0.2\omega$, $l/h = 0.6$. Stationary periodic vortex structures for (b) $\Omega = 0$, $q_0 = 0$, $q_1 = 0.75$ and for (c) $\Omega = 0.23\omega$, $q_0 = 0.4$, $q_1 = 0.9$. (d) Isolated vortex structures adjoining the channel walls at $\Omega = 0.09\omega$, $q_0 = 0.5$ and positioned with period $\lambda = 3.41$.

and the corresponding motion equations, (15), can be written as

$$\partial_t \eta_1 = -(\Omega - \omega)^{-1} \partial_x \frac{\delta H}{\delta \eta_1}, \qquad \partial_t \eta_2 = -(\omega - \Omega)^{-1} \partial_x \frac{\delta H}{\delta \eta_2}. \tag{84}$$

It is convenient to introduce non-dimensional variables and non-dimensional Hamiltonian:

$$q = \frac{\eta_2 - \eta_1}{2h}, \qquad s = \frac{\eta_2 + \eta_1}{2h}, \qquad \xi = \frac{x}{h}, \qquad \tau = t\frac{\omega - \Omega}{3}, \quad \tilde{H} = \frac{3}{2}(\omega - \Omega)^{-2} h^{-4} H,$$

whereby equations (84) can be rewritten as

$$\partial_\tau q = \partial_\xi \frac{\delta \tilde{H}}{\delta s}, \qquad \partial_\tau s = \partial_\xi \frac{\delta \tilde{H}}{\delta q}. \tag{85}$$

By expanding the hyperbolic functions in a power series and neglecting the terms higher than the second order derivatives with respect to ξ, we obtain the Hamiltonian in the large-scale approximation:

$$\begin{aligned}\tilde{H} = -\frac{1}{2}\int_{-\infty}^{+\infty} \Big\{ & q_\xi^2 \big[(1-q)^2(1+2q) + s^2\big(3q^2 - 2\big) + s^4\big] + s_\xi^2 q^2 \big[(1-q)^2 + 3s^2\big] \\ & + 4q_\xi s_\xi q s \big(1 - q^2 - s^2\big) - 3q^2\big(1 - s^2\big) + \frac{\omega - 2\Omega}{\omega - \Omega} q^2 - 3\frac{\omega}{\omega - \Omega} s^2 q \Big\} \, \mathrm{d}\xi. \end{aligned} \tag{86}$$

Let us suppose that the vortex structures are symmetric with respect to the channel axis so condition $s = 0$ is satisfied. Then, as Hamiltonian H does not contain terms linear in s, equations (85) are equivalent to equations

$$\partial_\tau q = 0, \qquad \partial_\xi \frac{\delta \tilde{H}}{\delta q} = 0. \tag{87}$$

Thus, the symmetric vortex structures are stationary formations and satisfy the nonlinear differential equation

$$q_\xi^2 (1-q)^2 (1+2q) = \beta q^3 - 3q^2 + \alpha_1 q + \alpha_0 = \beta (q - q_0)(q - q_1)(q - q_2). \tag{88}$$

Here, α_1 and α_0 are the constants of integration, $\beta = (\omega - 2\Omega)/(\omega - \Omega)$, and q_0, q_1, q_2 are the roots of the polynomial on the right-hand side of (88), so that

$$\beta(q_0 + q_1 + q_2) = 3. \tag{89}$$

Notice that since the turbulent Couette flow is simulated when $\omega > \Omega \geqslant 0$, the physical interest presents the following range of the parameter $1 \geqslant \beta > -\infty$.

Even more precise equations for describing the stationary vortex structures may be obtained if in the Hamiltonian expansion we take into account the terms of the higher order in Γ. Such Hamiltonian can be found directly from (83) at $\eta_1 = -\eta_2 = qh$ and has the following form

$$\tilde{H} = \frac{1}{2}\int_{-\infty}^{+\infty} \left\{ \frac{1}{2}\frac{\Omega + \omega}{\Omega - \omega} q^3 - \left[\cosh\Gamma - \cosh(1-q)\Gamma\right] \frac{3}{\Gamma^3 \cosh\Gamma} \sinh\Gamma q \right\} \mathrm{d}\xi.$$

It is easy to see that this Hamiltonian is a 'nonlocal' functional of q. However, in any finite order the perturbation theory leads to 'local' equations only approximately describing the vortex structures. Thus, for practical purposes, the perturbation theory is generally limited.

4.2. Stationary periodic vortex structures

In this section we return to the discussion of equation (88). The analysis reveals that equation (88) has physically meaningful solutions if all the roots, q_0, q_1 and q_2, are real. We commence with the case when all the q_i-roots are distinct. Without the loss of generality we assume that

$$0 \leqslant q_0 \leqslant q \leqslant q_1 \leqslant 1,$$

and q_0 and q_1 represent the upper and the lower bound of the solution, respectively. In this case, the corresponding solutions of (88) have an oscillating character and appear as strongly modulated vorticity-homogeneous layers. Such vortex structures are described by

$$q_\xi^2 = \frac{(q_1 - q)(q - q_0)[3 - \beta(q_0 + q_1 + q)]}{(1-q)^2(1+2q)}, \tag{90}$$

and represent periodic perturbations oscillating between q_0 and q_1 with the period

$$\lambda = 2\int_{q_0}^{q_1} \frac{(1-q)\sqrt{1+2q}\,\mathrm{d}q}{\sqrt{(q_0 - q)(q - q_1)[3 - \beta(q_0 + q_1 + q)]}}. \tag{91}$$

The shapes of the wave-like vortex structures are presented on *figures 4(b)* and *(c)*.

If $q_1 = 1$, this model allows for the existence of solitary vortex structures. In this case equation (88) takes the form

$$(1-q)\left\{(1-q)(1+2q)q_\xi^2 - (q - q_0)\left[3 - \beta(1 + q_0 + q)\right]\right\} = 0, \tag{92}$$

and has the solutions

$$q = 1, \qquad q_\xi^2 = \frac{(q - q_0)[3 - \beta(1 + q_0 + q)]}{(1-q)(1+2q)}. \tag{93}$$

Thus, a general solution represents a piecewise-continuous function obtained by ‘sewing’ together these solutions which may alternate arbitrarily or periodically. It can be seen in *figure 4(d)* that the solutions appear as isolated vortex structures adjoining the channel walls.

4.3. Effect of vortex structures on average velocity profile

Most real flows are complex dynamic regimes. Typically, only the average characteristics of such flows are known while the unperturbed state of the background flow is unknown. Such a lack of information about the initial perturbation-free state may be responsible for incorrect estimates of the role of the mechanisms in flow dynamics and interpretation of observable data. Therefore, in theoretical analysis, it is important to take into account all, if possible, models and scenarios which are capable of reproducing the average flow characteristics under observation (Pedlosky [18]). From this point of view, studying of how strongly-nonlinear dynamic regimes affect the average velocity profile in layer models is of special interest.

It is instructive to assess the influence of the periodic vortex structures considered above on the average profile of Couette flow. Taking into account the model symmetry, it is sufficient to consider only the upper half of the channel in calculating the average flow characteristics. Adhering to this rule, first we find the vorticity distribution in the perturbed flow:

$$\omega(\zeta,\xi) = \Omega\theta\big[q(\xi)-\zeta\big] + \omega\theta\big[\zeta - q(\xi)\big], \tag{94}$$

where $\zeta = z/h$ is the dimensionless vertical coordinate, θ is theta-function:

$$\theta(x) = \begin{cases} 1, & x \geqslant 0; \\ 0, & x < 0. \end{cases}$$

Average vorticity $\bar{\omega}(\zeta)$ can be easily derived from (94) under the assumption that q is a periodic function of ξ with period λ. Then, by averaging expression (94) over the period λ, we obtain

$$\bar{\omega}(\zeta) = \frac{1}{\lambda}\int_0^\lambda \big(\Omega\theta\big[q(\xi)-\zeta\big] + \omega\theta\big[\zeta - q(\xi)\big]\big)\,\mathrm{d}\xi = \Omega + \frac{\omega-\Omega}{\lambda}\int_0^\lambda \theta\big[\zeta - q(\xi)\big]\,\mathrm{d}\xi. \tag{95}$$

Since velocity u and vorticity $\bar{\omega}$ are related as $\mathrm{d}u/\mathrm{d}z = -\bar{\omega}$, the average velocity profile is found according to the formula:

$$u(\zeta) = -h\int_0^\xi \bar{\omega}(\zeta')\,\mathrm{d}\zeta' = -h\Omega\zeta + \frac{h(\Omega-\omega)}{\lambda}\int_0^\lambda \big(\zeta - q(\xi)\big)\theta\big[\zeta - q(\xi)\big]\,\mathrm{d}\xi. \tag{96}$$

For numerical calculations it is more convenient to rewrite the integral on the right-hand side of (96) as

$$u(\zeta) = \begin{cases} -h\Omega q_0 + f(q_0) + h\omega(q_0-\zeta), & q_0 \leqslant \zeta \leqslant 1; \\ -h\Omega\zeta + f(\zeta), & q_1 \leqslant \zeta \leqslant q_0; \\ -h\Omega\zeta, & 0 \leqslant \zeta \leqslant q_1; \end{cases} \tag{97}$$

where

$$f(\zeta) = \frac{2h(\Omega-\omega)}{\lambda}\int_{q_1}^{\zeta} \frac{(\zeta-q)(1-q)\sqrt{1+2q}\,\mathrm{d}q}{\sqrt{(q_0-q)(q-q_1)[3-\beta(q_0+q_1+q)]}}. \tag{98}$$

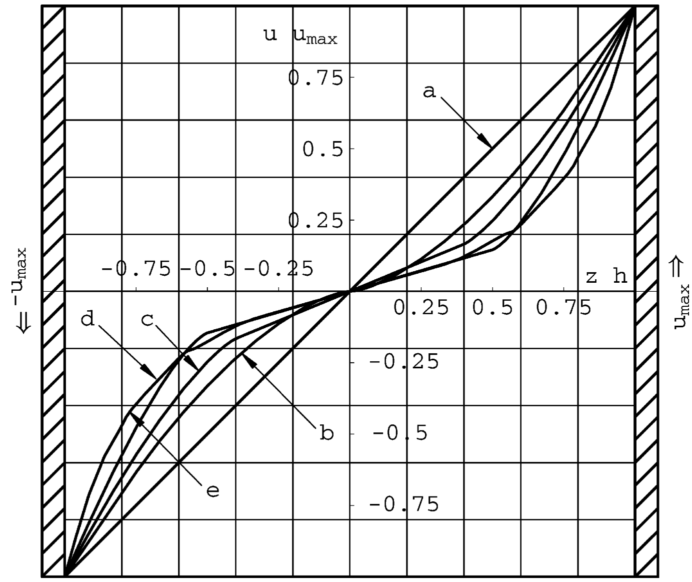

Figure 5. Average velocity profiles normalized to unit in maximum: (a) the velocity profile of laminar Couette flow. The profiles (b), (c) and (d) correspond to the flows disturbed by vortex structures represented in *figure 4(b), (c)* and *(d)*. (e) The velocity profile of turbulent Couette flow at Reynolds number $Re = 2900$ ([19]).

The results are obtained through the numerical integration of (98) and are presented in *figure 5* which demonstrates the average velocity profiles normalized to a unit at their maximum. Each profile corresponds to the flow (disturbed) by the vortex structures described in *figure 4*. For a comparison, in *figure 5* we present the profiles of a laminar and a turbulent Couette flow with Reynolds number $Re = 2900$ (Schlichting [19]).

5. Conclusion

The development (see Goncharov and Pavlov [5,6]) of the fundamental theoretical method – the Hamiltonian Approach – would remain incomplete if no practical application of the theoretical analysis were given. In this paper we applied the method to important physical problems – large-scale vortex structures in shear flows. Such models describing many typical natural flows are of special interest to atmospheric and planetary physicists, meteorologists, and specialists in fluid dynamics.

The application of the Hamiltonian Approach to Poiseuille-type and Couette-type flows allowed us to describe and classify isolated, long-lasting vortex structures appearing in the flows under different regimes. We also analyzed the effect of vortex structures on the average velocity profile of the flows. This theoretical result is informative for experimental studies. Typically only the averaged characteristics of the perturbed flows are observed while the unperturbed state of the background flow is unknown, thus making interpretation of observable data less reliable.

The Hamiltonian formulation developed in the works of Goncharov and Pavlov [5,6] is very convenient for analyzing such flows. It focuses on a single quantity – the Hamiltonian – rather than multiple dynamic equations, and thus minimizes analytical manipulations. The formalism also allows one to overcome the barrier of weak nonlinearity.

In general, the precise expression for the Hamiltonian and the structure of the corresponding equations of motion in concrete situations are not as trivial as they may appear at first glance. Indeed, in order to correctly capture the specifics of each practical problem, the proper form of the Hamiltonian and the motion equation must be derived at the very beginning of the analysis.

Finally, the need to use approximate analytical (asymptotical) or numerical methods imposes special requirements on the structure of the essential element of the Hamiltonian Approach – the Poisson bracket (see, Goncharov and Pavlov [6]). Obviously, these methods are realized with more ease in the framework of the Hamiltonian (canonical) formulation with the Poisson tensor independent of field variables. In this case, the only object for approximation is the Hamiltonian, which eliminates the need to perform multiple, cumbersome and recurrent calculations replicated according to the number of equations. It should be kept in mind that formal applications of finite-difference methods to systems of traditional hydrodynamic equations (typically written in non-canonical form) can lead to violation of the conservation laws. In all such cases the loss of conservativity leads to non-physical consequences. Such a loss of conservativity is a result of the loss of the Jacobi property and may occur without any external physical reasons, but rather due to the finite-difference scheme only. This remark is of particular significance because theoretical and computing physics widely uses discrete numerical schemes. In this light this Hamiltonian reformulation of the hydrodynamical description should be considered as one of most methodologically developed version of the Hamiltonian formalism not only satisfying the requirement of the simplicity of the structure, but also providing standardized means to solve various fluid dynamics problems.

Acknowledgment

This work was partially supported by the Russian Fundamental Research Foundation under grant No. 00-05-64019. V.G. expresses his gratitude to the UFR of Pure and Applied Mathematics, to the Department of Fundamental Mechanics (University of Lille 1, France) and to Laboratoire de Mécanique de Lille for its hospitality during his visit to Lille when most of this research was carried out. The authors are grateful to the anonymous referees for useful remarks.

References

[1] Zabusky N.J., Huges M.H., Roberts K.V., Contour dynamics for the Euler equations in two-dimensions, J. Comput. Phys. 30 (1979) 96–106.
[2] Saffman P.G., Vortex Dynamics, Cambridge University Press, 1992.
[3] Dritschel D.G., Contour dynamics/surgery on the sphere, J. Comput. Phys. 79 (1988) 477–483.
[4] Dritschel D.G., McIntyre M.E., Does contour dynamics go singular?, Phys. Fluids A 2 (5) (1990) 748–753.
[5] Goncharov V.P., Pavlov V.I., Problems of Hydrodynamics in Hamiltonian Approach, Moscow University Press, Moscow, 1993 (in Russian).
[6] Goncharov V.P., Pavlov V.I., Some remarks on the physical fundamentals of the Hamiltonian description of fluid motions, Eur. J. Mech. B-Fluids 16 (4) (1997) 509–555.
[7] Arnold V.I., The Hamiltonian nature of the Euler equations in the dynamics of a rigid body and of a perfect fluid, Russ. Math. Surv. 24 (3) (1969) 225–226.
[8] Morrison P.J., Poisson brackets for fluid and plasmas, in: Am. Inst. Phys. Conf. Proc. 88 (1982) 13–46.
[9] Morse P.M., Feshbach H., Methods of Theoretical Physics, part I, McGraw-Hill, 1953.
[10] Maslov V.P., Operational Methods, Nauka, Moskow, 1973.
[11] Pullin D.I., The nonlinear behavior of a constant vorticity layer at a wall, J. Fluid Mech. 108 (1981) 401–421.
[12] Marsden J.E., Weinstein A., Coadjoint orbits, vortices and Clebsch variables for incompressible fluids, Physica D 7 (1983) 305–323.
[13] Abramovitz M., Stegun I.A., Handbook of Mathematical Functions, U.S. Govt. Printing Office, Washington, D.C., 1964.
[14] Goncharov V.P., Vortex structures in shear flows, Izv. Acad. Sci. USSR Mech. Zhid. Gaza 2 (1986) 65–75 (in Russian).
[15] Landau L.D., Lifshitz E.M., Fluid Mechanics, 2nd ed., Pergamon Press, Oxford, New York, 1987.
[16] Kantwell G., Organizovannye dvijenija v turbulentnykh potokakh, in: Vikhri i Vilny, Moscow, Mir, 1984, pp. 9–79.
[17] Milne-Thomson L.M., Theoretical Hydrodynamics, 5th ed., MacMillan, London, 1968.
[18] Pedlosky J., Geophysical Fluid Dynamics, 2nd ed., Springer-Verlag, New York, 1987.
[19] Schlichting H., Boundary Layer Theory, McGraw-Hill, 1955.